Supplement of The Cryosphere, 18, 2809–2830, 2024
https://doi.org/10.5194/tc-18-2809-2024-supplement

The Cryosphere Open Access EGU

Supplement of

Mapping and characterization of avalanches on mountain glaciers with Sentinel-1 satellite imagery

Marin Kneib et al.

Correspondence to: Marin Kneib (marin.kneib@gmail.com)

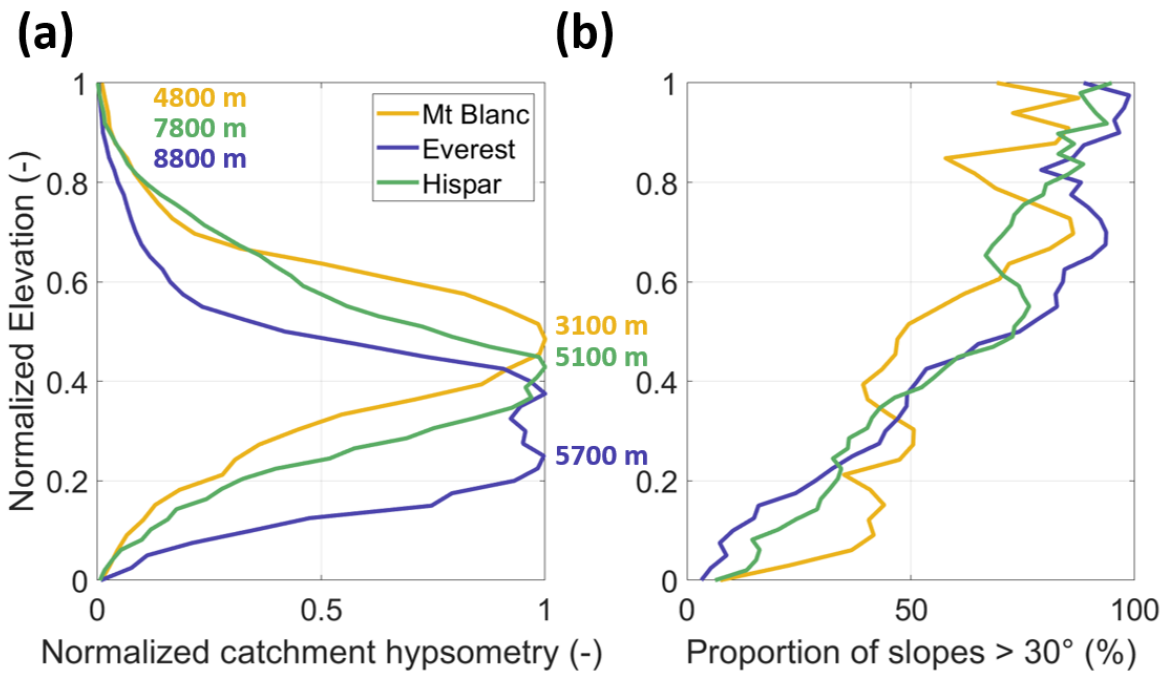

Figure S1: (a) Hypsometry of all glacier catchments of the three survey domains and (b) their proportion of slopes steeper than 30° per elevation bands.

Table S1: Sentinel-1 RGB scenes used for the manual outline comparison between the four independent operators, along with the F1-scores relative to the manual outlines of the first operator, responsible for the delineation of all outlines used for the calibration.

Site	Orbit	Date range	F1-score Op. 2	F1-score Op. 3	F1-score Op. 4
Mt. Blanc	Ascending	08/12/19 - 14/12/19	0.54	0.66	0.60
		30/05/20 - 05/06/20			
	Descending	07/12/19 - 13/12/19			
		29/05/20 - 04/06/20			
Everest	Ascending	08/03/20 - 20/03/20			
		11/08/20 - 23/08/20			
	Descending	04/03/20 - 16/03/20			
		07/08/20 - 19/08/20			

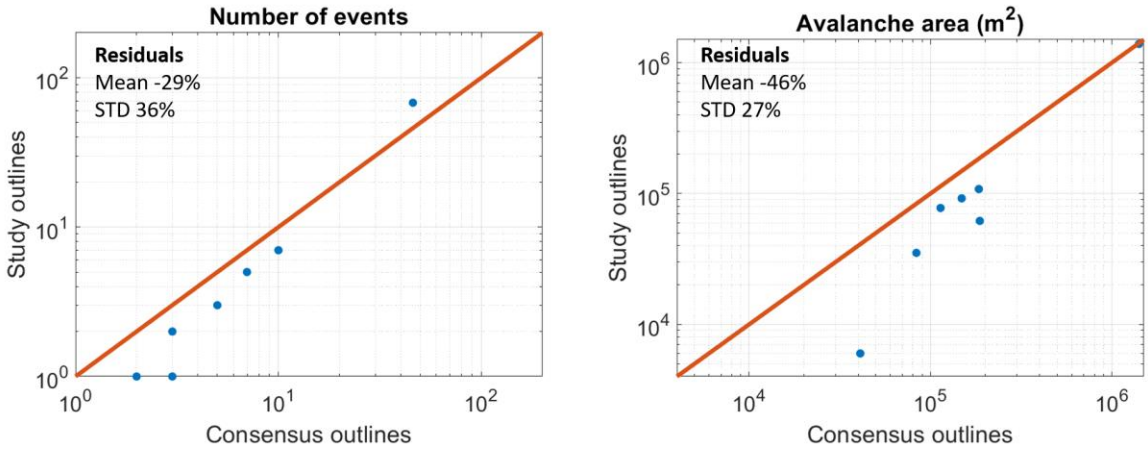

Figure S2: avalanche number and relative area of this study outlines versus those of the consensus outlines (blue dots), in comparison with the 1:1 line (red). Each dot corresponds to one of the eight Sentinel-1 image pairs used for this intercomparison exercise.

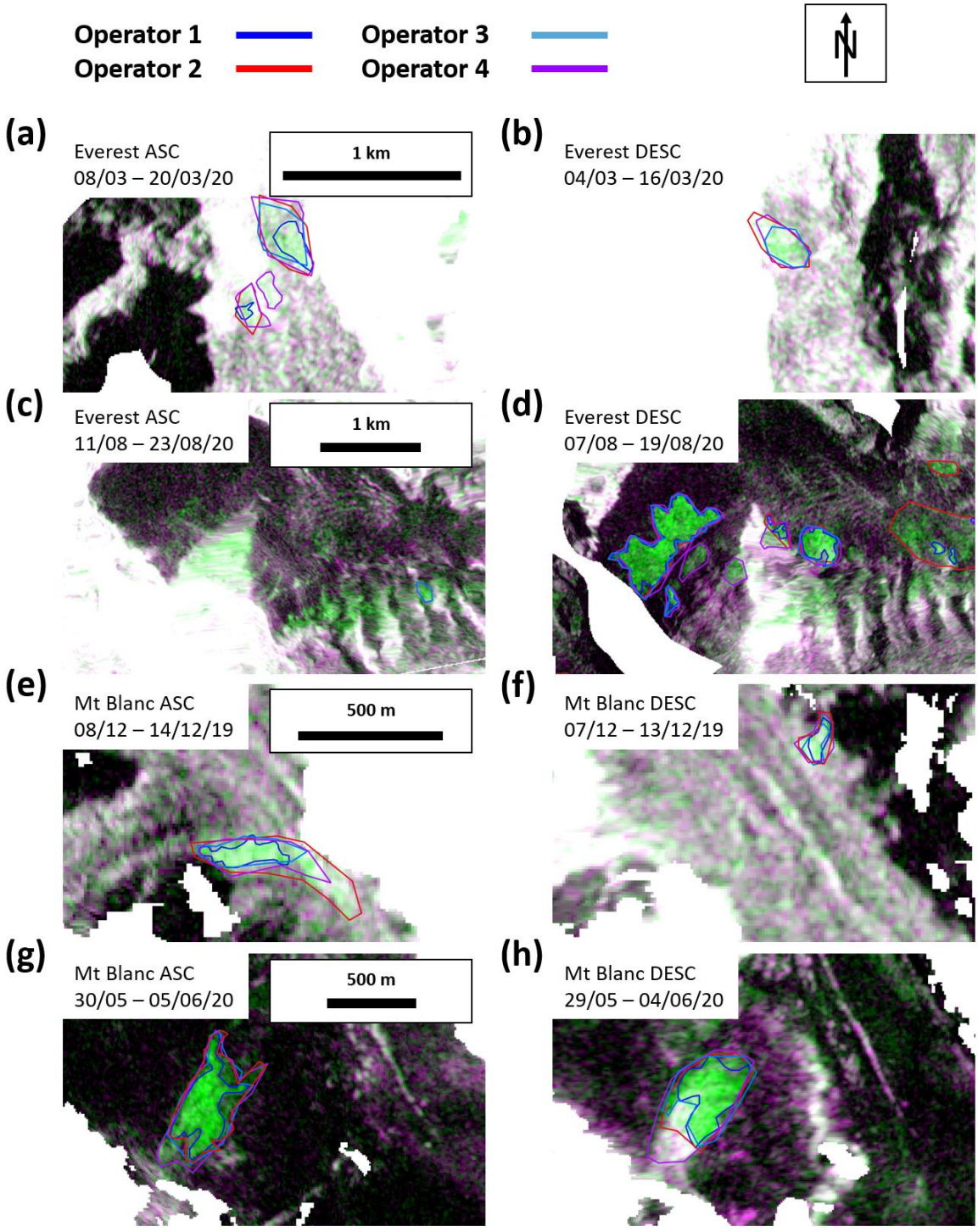

Figure S3: Comparison examples of manual outlines from four independent operators. The left panels show ascending scenes, and the right panels show the exact same extents for the contemporaneous descending scenes. Operator 1 was responsible for deriving the entire calibration dataset. The different RGB bands range between -25 and -6 dB.

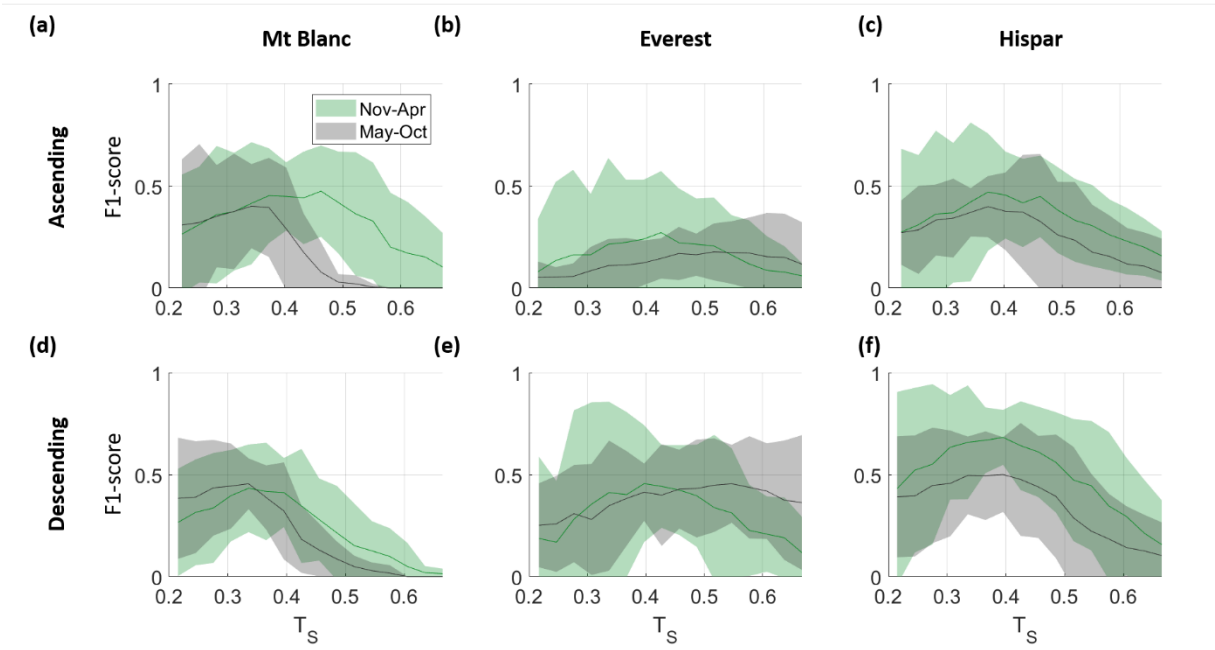

Figure S4: Mean value +/- 3 standard deviations of F1-score as a function of values of TS taken between 0.2 and 0.65 for ascending and descending orbits of all three survey areas.

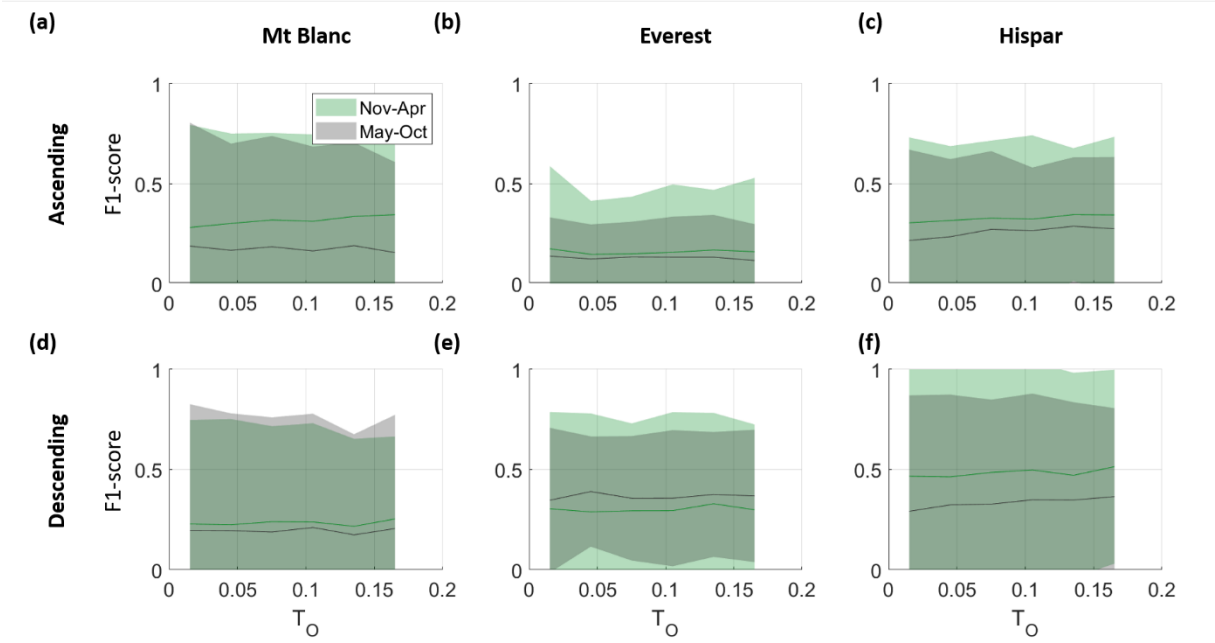

Figure S5: Mean value +/- 3 standard deviations of F1-score as a function of values of T_O for ascending and descending orbits of all three survey areas.

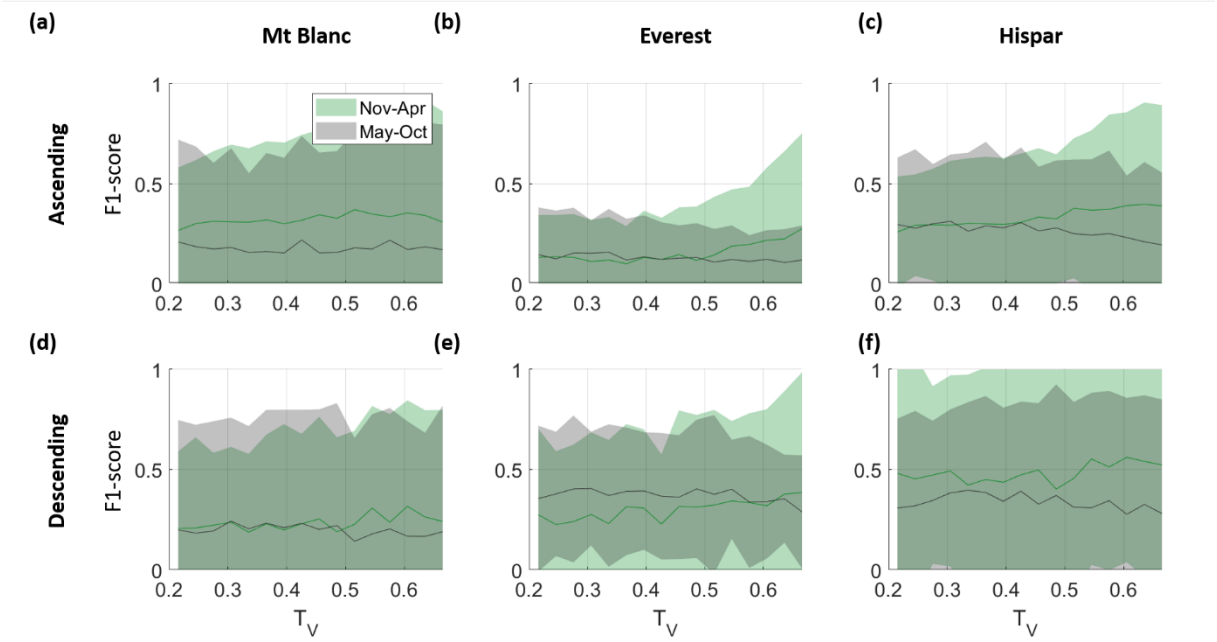

Figure S6: Mean value +/- 3 standard deviations of F1-score as a function of values of T_V for ascending and descending orbits of all three survey areas.

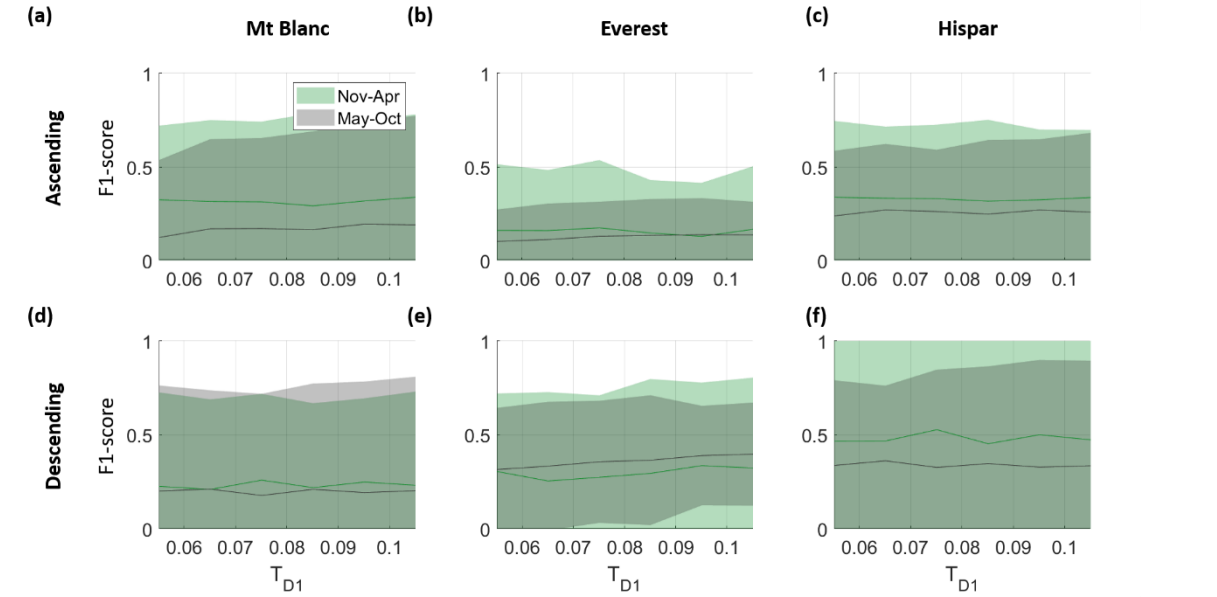

Figure S7: Mean value +/- 3 standard deviations of F1-score as a function of values of T_{D1} for ascending and descending orbits of all three survey areas.

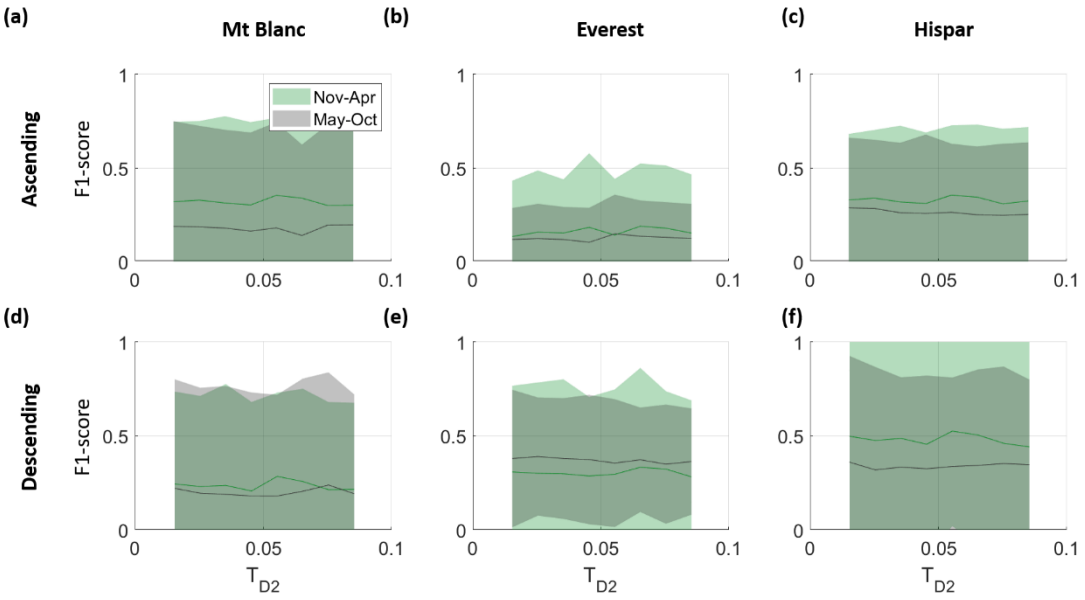

Figure S8: Mean value +/- 3 standard deviations of F1-score as a function of values of T_{D2} for ascending and descending orbits of all three survey areas.

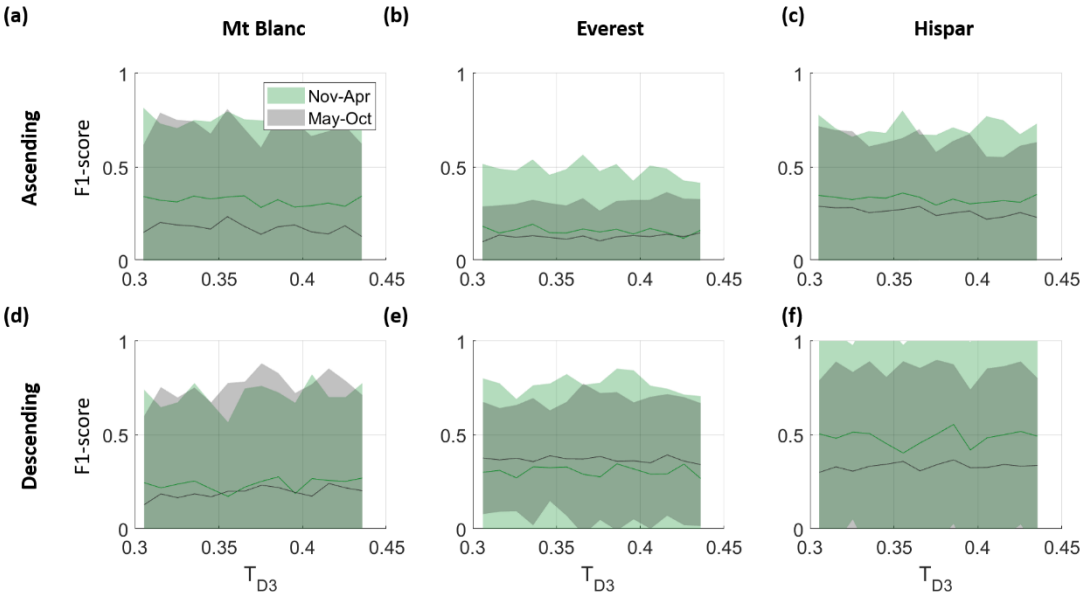

Figure S9: Mean value +/- 3 standard deviations of F1-score as a function of values of T_{D3} for ascending and descending orbits of all three survey areas.

α = Projected local incidence angle
dh = Elevation change since 2000
S = Shift

$$S = dh \times \tan(\alpha)$$

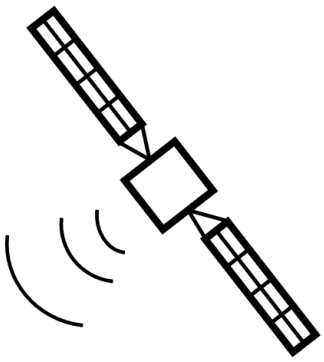

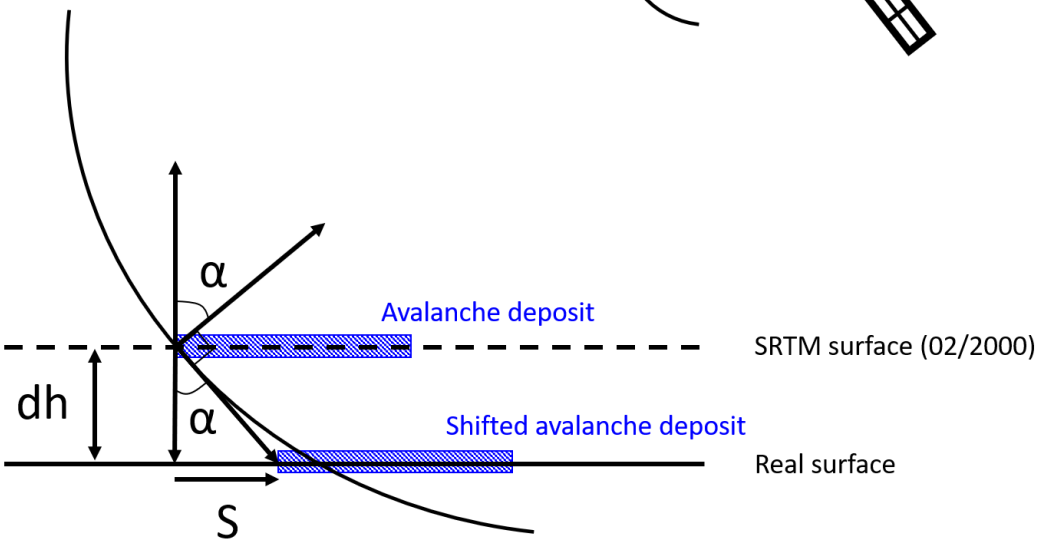

Figure S10: Accounting for surface lowering to shift avalanche outlines from Sentinel-1 images projected on the SRTM DEM acquired in February 2000.

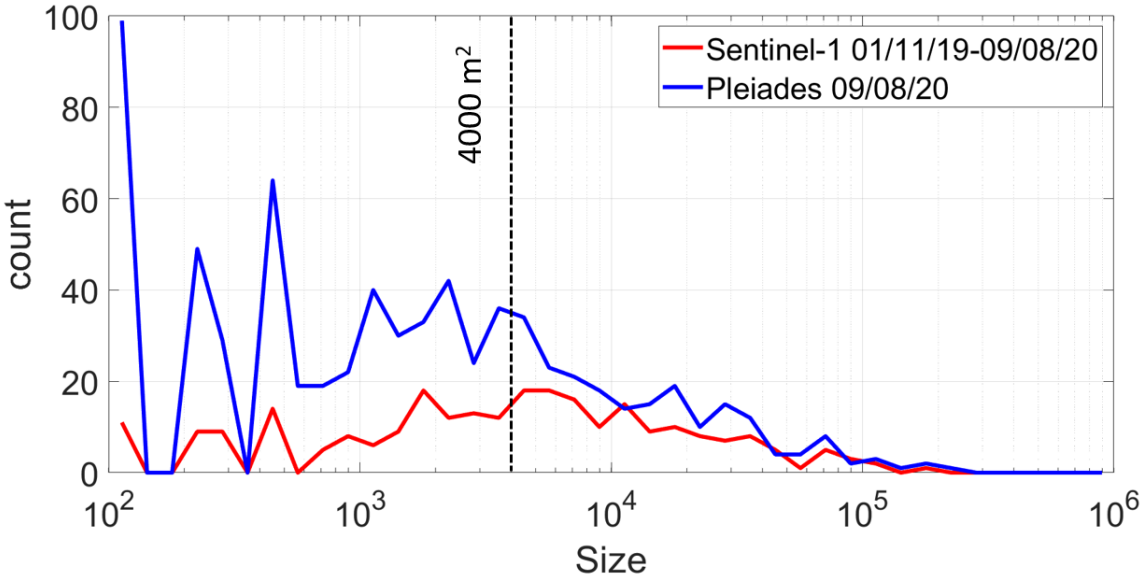

Figure S11: Size comparison of the aggregation of all Sentinel-1 deposits (ascending and descending orbits) for the period 01/11/2019-09/08/2020 with all deposits identifiable in the 09/08/2020 Pléiades orthoimage.

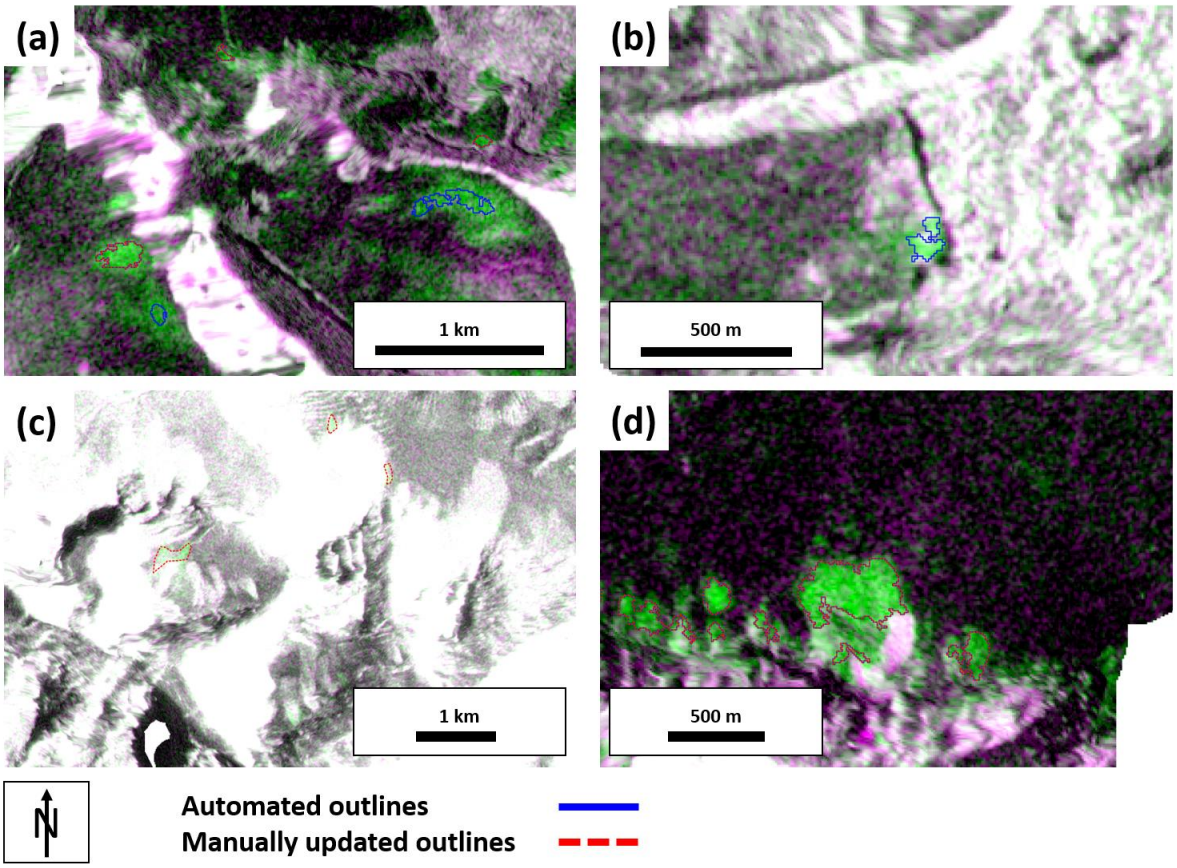

Figure S12: (a) False positive detections caused by snow wetness changes, Khumbu RGB composite of 03/09/2018-15/09/2018. (b) False positive decisions caused by calving at the surface of a proglacial lake, Khumbu RGB composite of 02/01/2018-14/01/2018. (c) False negative detections of bright deposits, Hispar RGB composite of 03/12/2017-15/12/2017. (d) Partial detection of avalanche deposits, with an older deposit visible in light purple, Hispar RGB composite 04/09/2018-16/09/2018. The different RGB bands range between -25 and -6 dB.

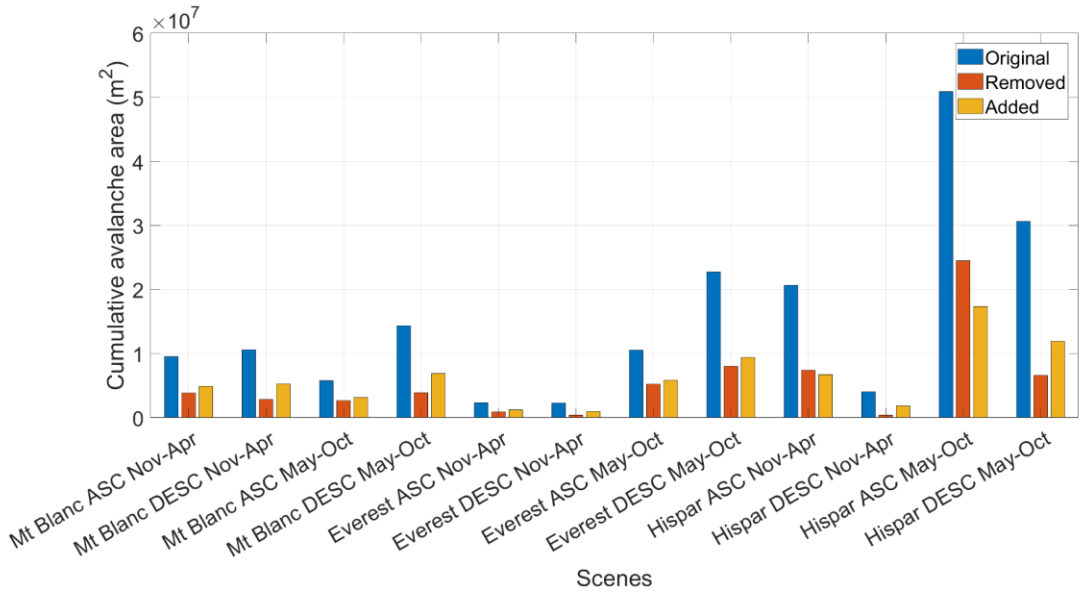

Figure S13: Automatically derived avalanche area across all Sentinel-1 RGB scenes (blue) versus the area that was manually removed (red) and manually added (yellow).

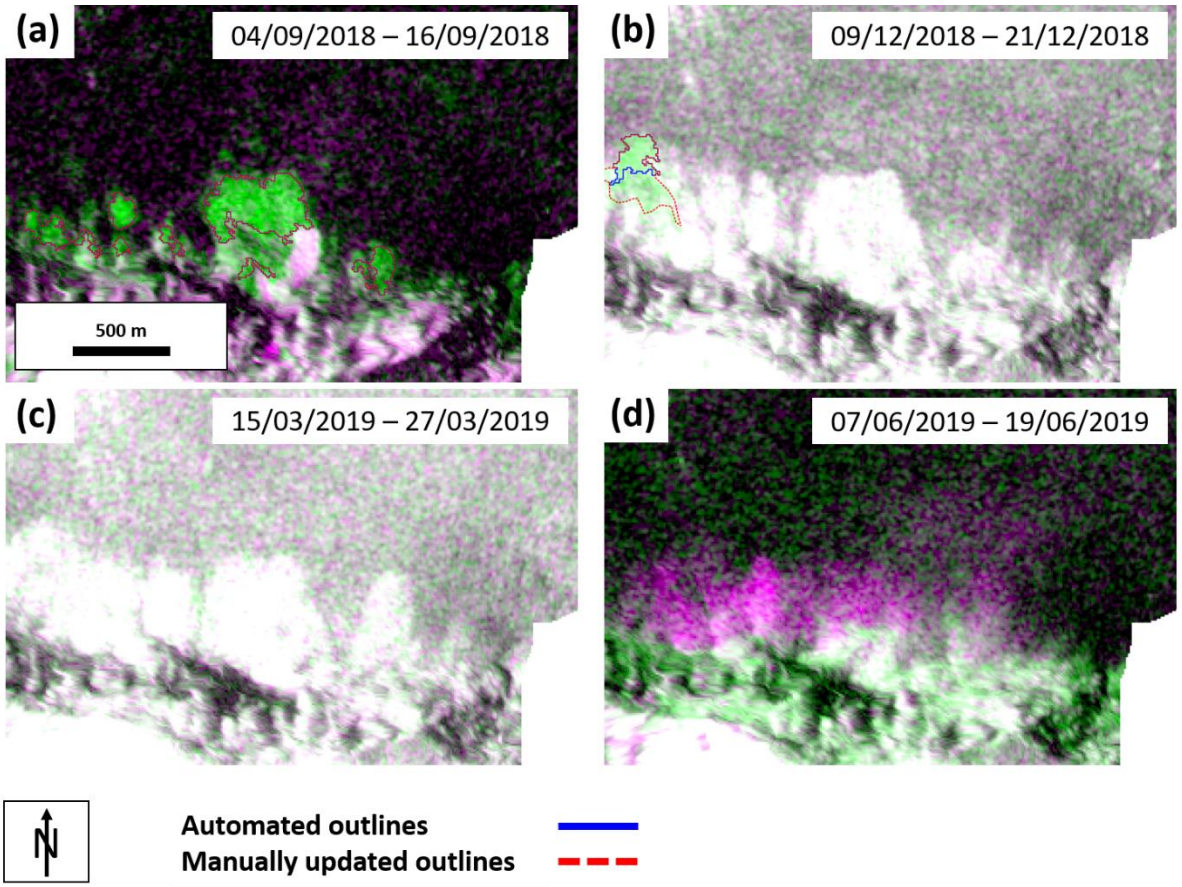

Figure S14: (a) Detection of avalanche deposits, with an older deposit visible in light purple, Hispar RGB composite 04/09/2018-16/09/2018. The high backscatter values from these avalanche deposits remained visible until 19/06/2019 (b-d). The different RGB bands range between -25 and -6 dB.

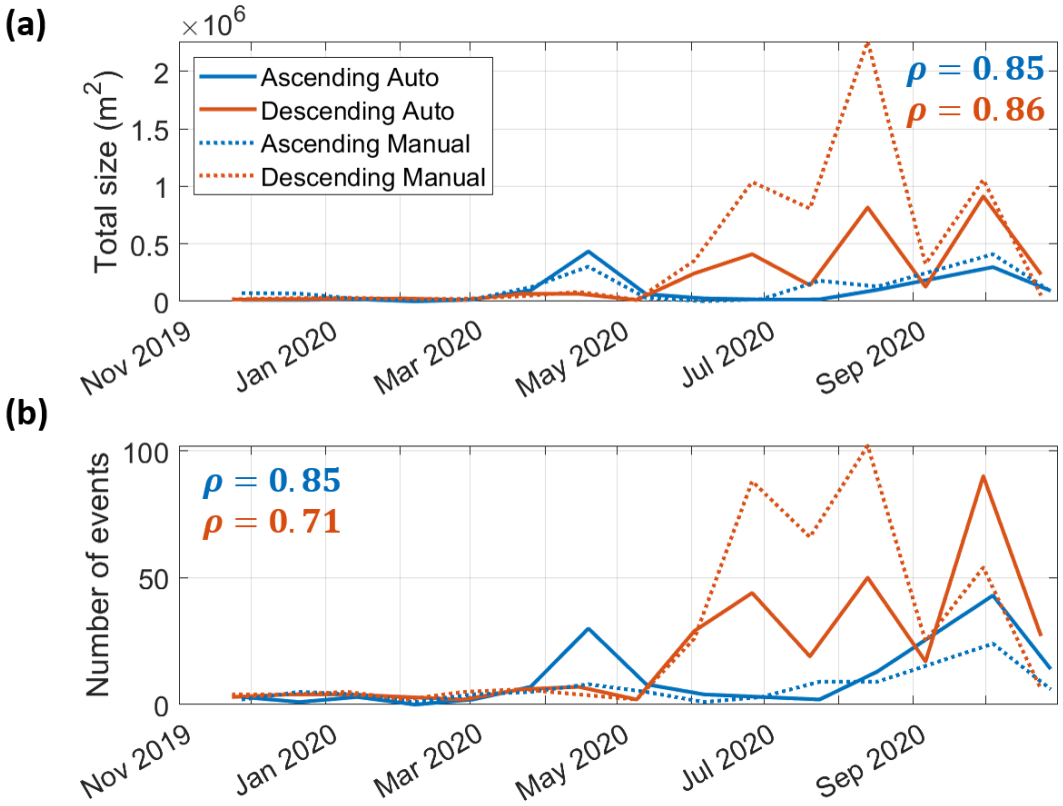

Figure S15: Total size and number of manually and automatically detected avalanche events as a function of time for the period 11/2019-10/2020 for the validation datasets of Everest. The Pearson's correlation coefficients are indicated in blue (ascending) and red (descending).

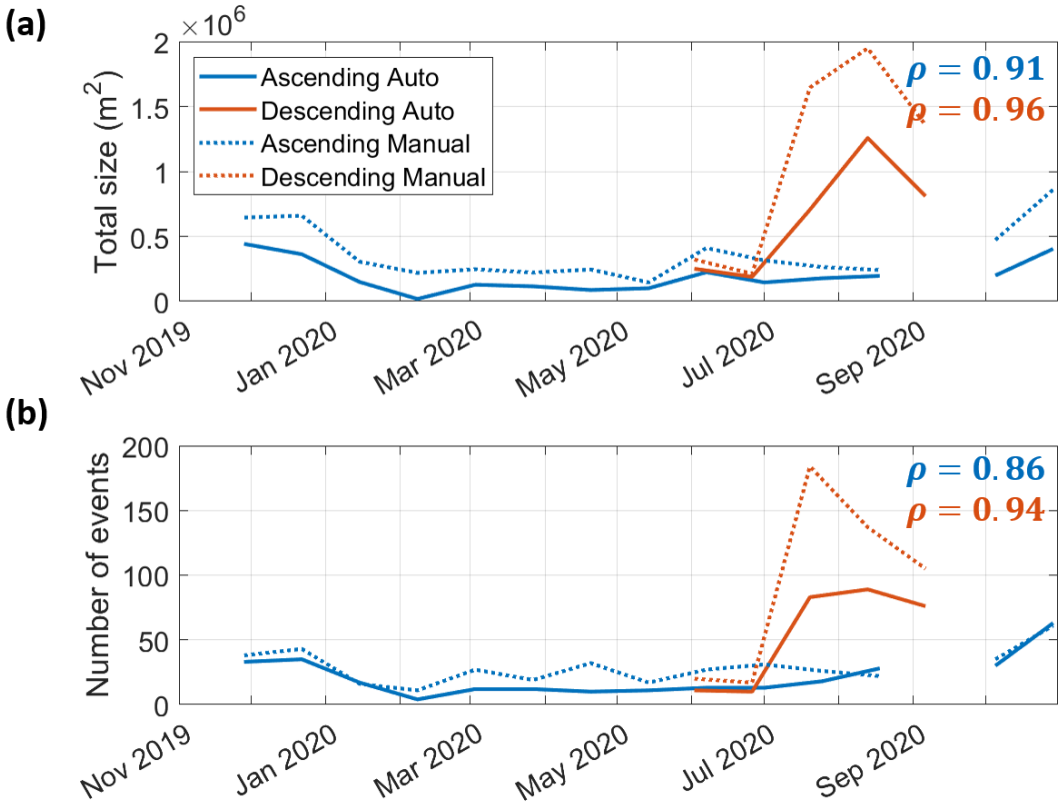

Figure S16: Total size and number of manually and automatically detected avalanche events as a function of time for the period 11/2019-10/2020 for the validation datasets of Hispar. The Pearson's correlation coefficients are indicated in blue (ascending) and red (descending).

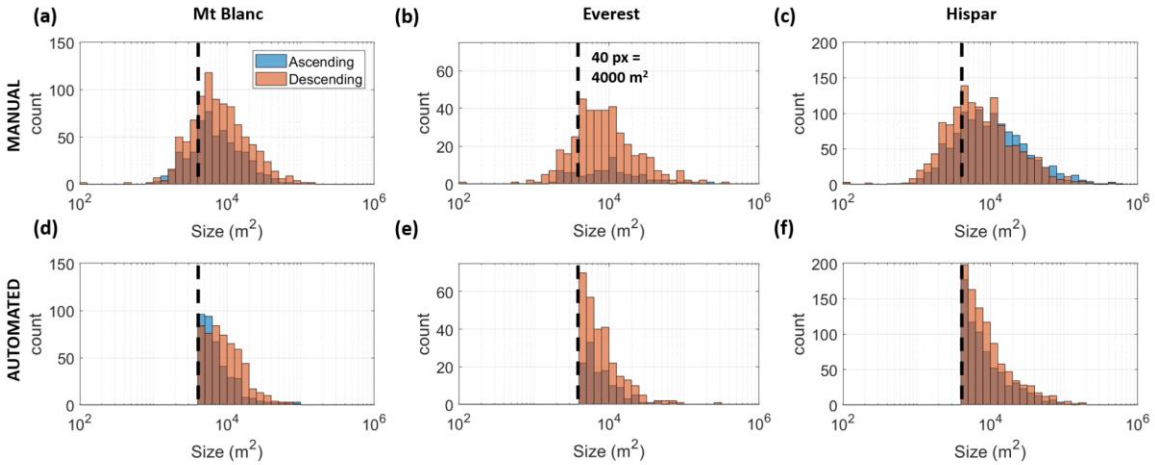

Figure S17: Size distribution of the avalanche deposits derived manually (a-c) and automatically (d-e) for all survey domains over the period 11/2019-10/2020 for the validation datasets of the three survey domains, split between ascending (blue) and descending (red) orbits. The vertical dashed lines indicate the 40-pixel (4000 m^2) threshold used as a minimal size, and below which individual deposits are hard to detect, as shown by the decrease in detection below this threshold.

Table S2: ratio of false positive and false negative detections obtained when applying the Mt Blanc 6 days sets of parameters to the Mt Blanc 12 days sets of images.

FP/FN			Mt Blanc (6 days)			
			DESC		ASC	
			N-A	M-O	N-A	M-O
Mt Blanc (12 days)	DESC	Nov-Apr	**1.41**	1.75	0.78	0.82
		May-Oct	2.72	**2.24**	0.42	0.83
	ASC	Nov-Apr	4.58	5.55	**2.61**	3.00
		May-Oct	3.77	3.01	0.73	**1.35**

Table S3: results obtained when fitting an exponential decrease of the form $Y = e^{Ax}$ to the normalised size distributions of avalanches (Fig. 8b).

Survey area	Orbit	A (m^{-2})	R^2
Mt Blanc	Ascending	-2.3×10^{-5}	0.56
	Descending	-2.6×10^{-5}	0.89
Everest	Ascending	-2.1×10^{-5}	0.81
	Descending	-1.9×10^{-5}	0.55
Hispar	Ascending	-1.1×10^{-5}	0.49
	Descending	-1.6×10^{-5}	0.44

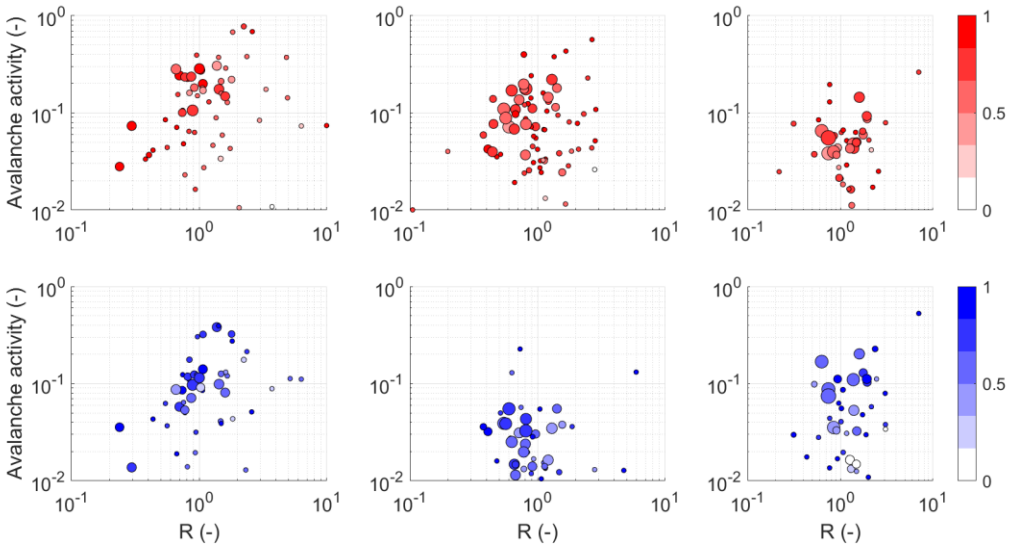

Figure S18: Avalanche activity per glacier as a function of the proportion of slopes steeper than 30° in the glaciers' catchments (R index, Hughes, 2008). The size of the dots indicates the size of the glaciers and their colour corresponds to the proportion of glacier area that is free of shadow and layover.

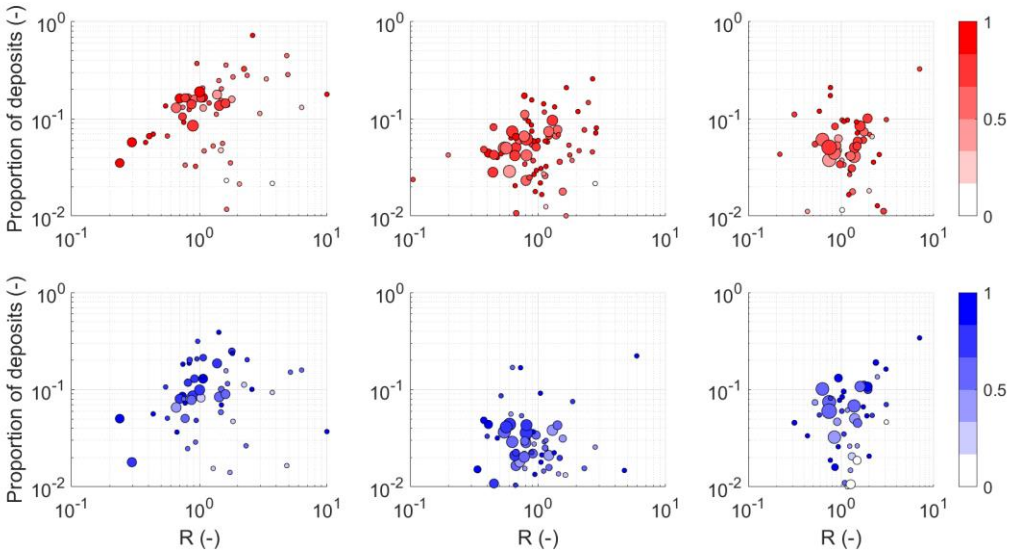

Figure S19: Proportion of deposits per glacier as a function of the proportion of slopes steeper than 30° in the glaciers' catchments (R index, Hugues, 2008). The size of the dots indicates the size of the glaciers and their colour corresponds to the proportion of glacier area that is free of shadow and layover.

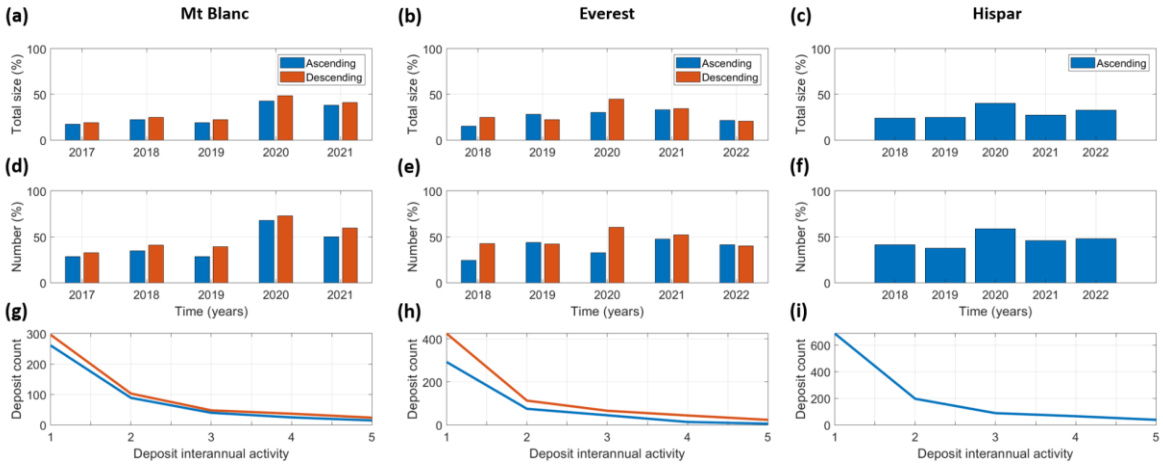

Figure S20: Deposit activity for each hydrological year. (a-c) Area size of yearly deposits relative to the area size of all deposits for the three survey domains. (d-f) Number of active deposits each year relative to the total number of deposits over five years. (g-i) Number of years (out of five) when the deposits counted at least one avalanche event.

Table S4: relative number (total size) of avalanches for each orbit of each survey domain per season over the five-year study period. The Hispar descending scenes were not accounted for due to important data gaps in the time series.

Survey area	Orbit	Winter	Spring	Summer	Autumn
Mt Blanc	Ascending	35% (33%)	32% (34%)	9% (9%)	24% (23%)
	Descending	21% (22%)	44% (44%)	15% (16%)	19% (17%)
Everest	Ascending	5% (4%)	22% (26%)	45% (46%)	28% (25%)
	Descending	3% (3%)	11% (10%)	53% (53%)	32% (35%)
Hispar	Ascending	18% (11%)	30% (24%)	37% (51%)	15% (15%)

Table S5: relative precipitation amount for each survey domain over the five-year study period.

Survey area	Winter	Spring	Summer	Autumn
Mt Blanc	31%	22%	23%	24%
Everest	5%	20%	69%	5%
Hispar	26%	25%	27%	23%

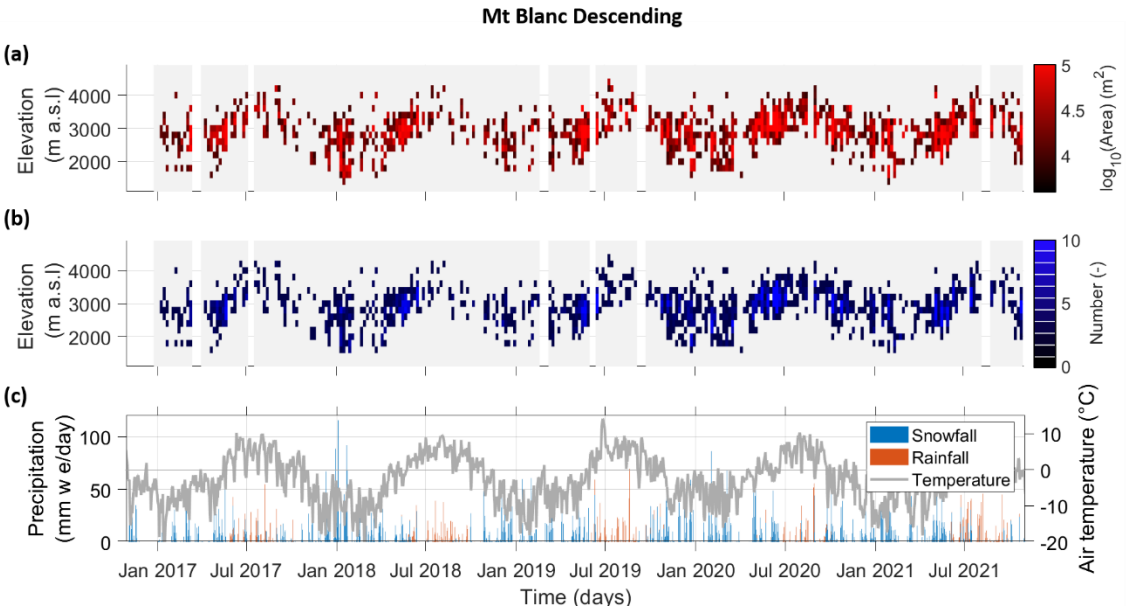

Figure S21: Five years (11/2016-10/2021) of avalanche time series over the Mt Blanc massif in the descending orbits. (a) Total area and (b) number of avalanches as a function of time and elevation. Frequency of acquisitions is 6 days. White rectangles indicate data gaps. (c) Total precipitation and mean daily air temperature at 3000 m a.s.l over the Mt Blanc massif according to the SAFRAN reanalysis product (Vernay et al., 2022).

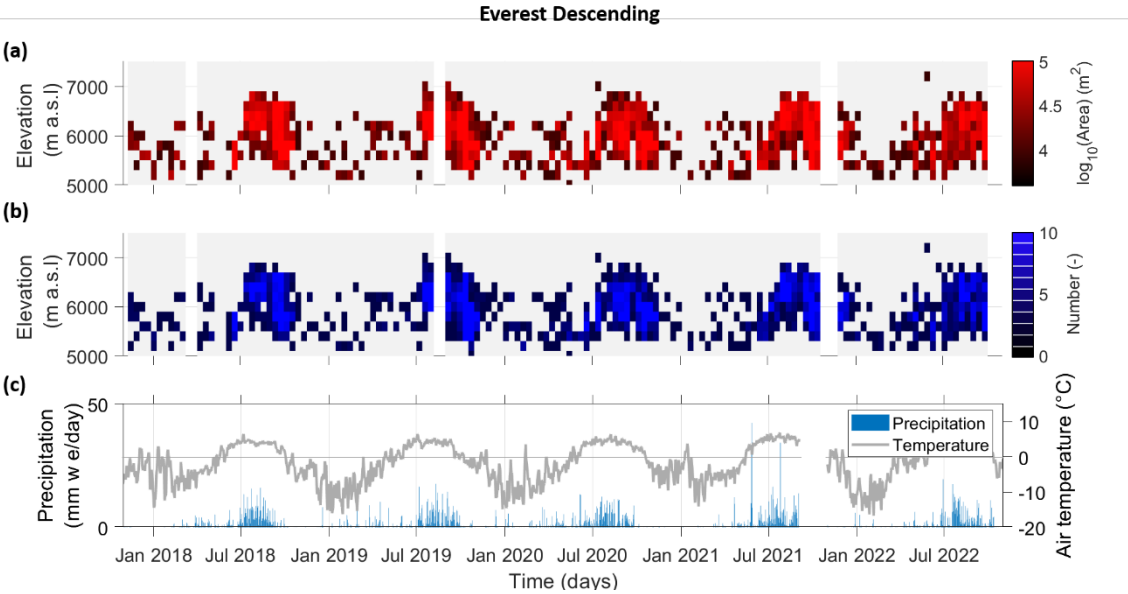

*Figure S22: Five years (11/2017-10/2022) of avalanche time series over the Everest region in the descending orbits. (a) Total area and (b) number of avalanches as a function of time and elevation. Frequency of acquisitions is 12 days. White rectangles indicate data gaps. (c) Daily precipitation and mean air temperature recorded at the Pyramid precipitation gauge (*5035 m a.s.l*).*

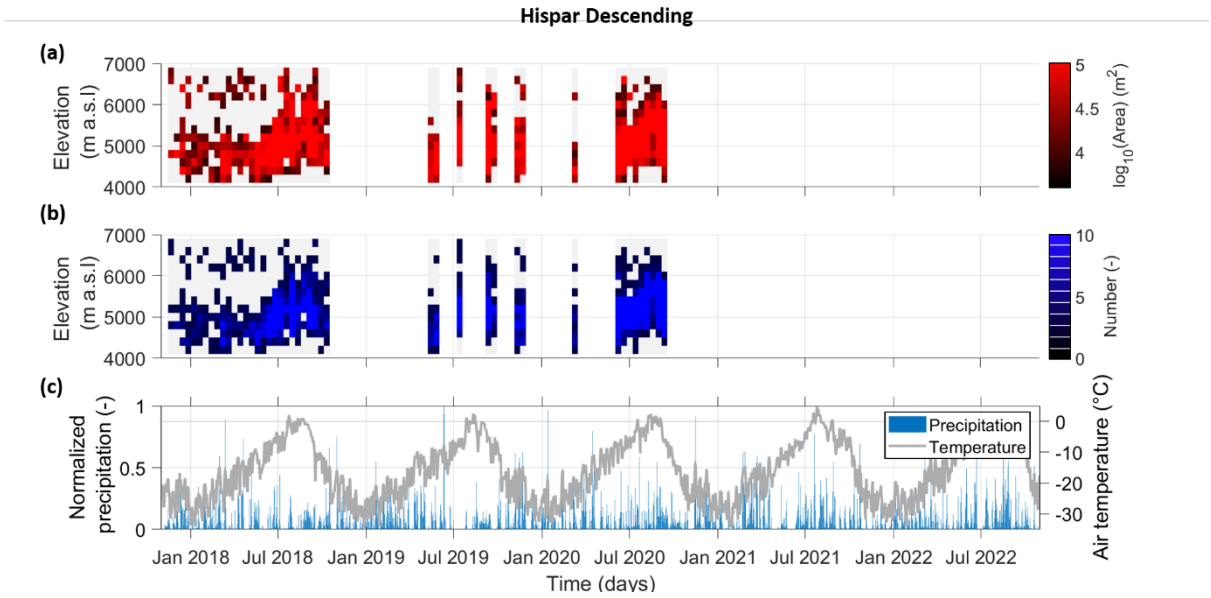

Figure S23: Five years (11/2017-10/2022) of avalanche time series over the Hispar region in the descending orbits. (a) Total area and (b) number of avalanches as a function of time and elevation. Frequency of acquisitions is 12 days. White rectangles indicate data gaps. (c) Daily precipitation and mean air temperature over the region from the ERA5-Land reanalysis product (Muñoz Sabater, 2019). Daily precipitation values were normalised due to potential biases (Khadka et al., 2022).

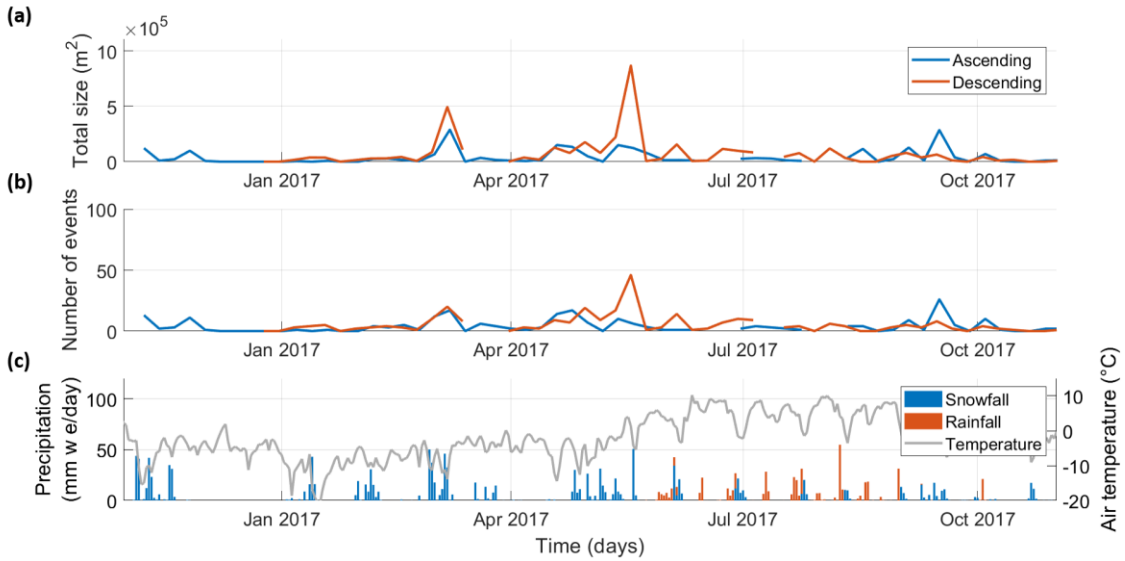

Figure S24: One year (11/2016-10/2017) of avalanche time series over the Mt Blanc massif in the ascending and descending orbits. (a) Total area and (b) number of avalanches as a function of time across all elevations. (c) Total daily precipitation and mean daily air temperature at 3000 m a.s.l over the Mt Blanc massif according to the SAFRAN reanalysis product (Vernay et al., 2022). The avalanche danger level was not available for this period.

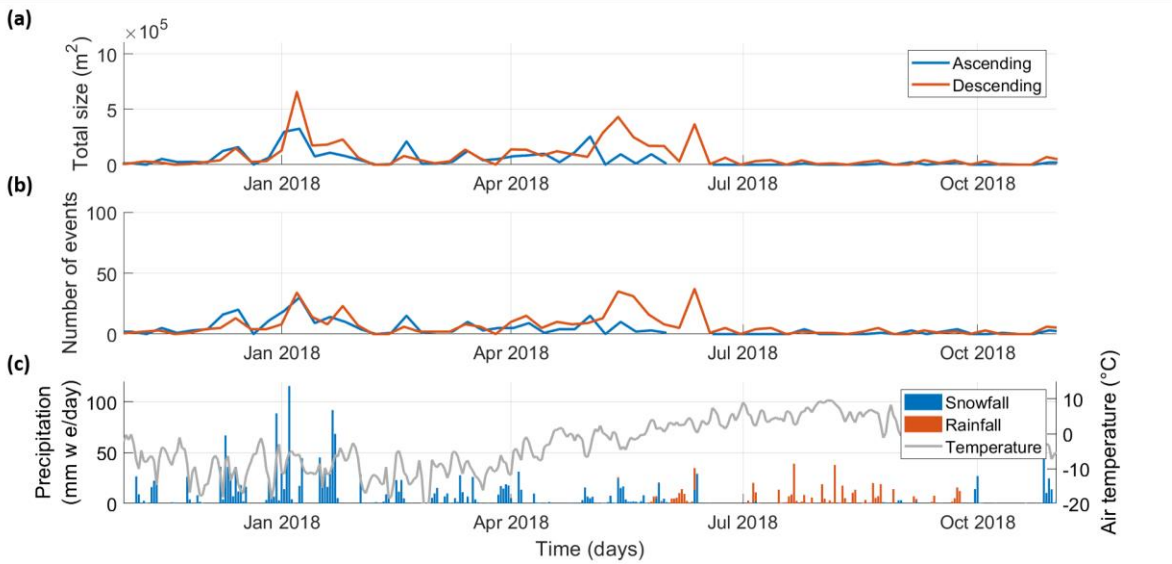

Figure S25: One year (11/2017-10/2018) of avalanche time series over the Mt Blanc massif in the ascending and descending orbits. (a) Total area and (b) number of avalanches as a function of time across all elevations. (c) Total daily precipitation and mean daily air temperature at 3000 m a.s.l over the Mt Blanc massif according to the SAFRAN reanalysis product (Vernay et al., 2022). The avalanche danger level was not available for this period.

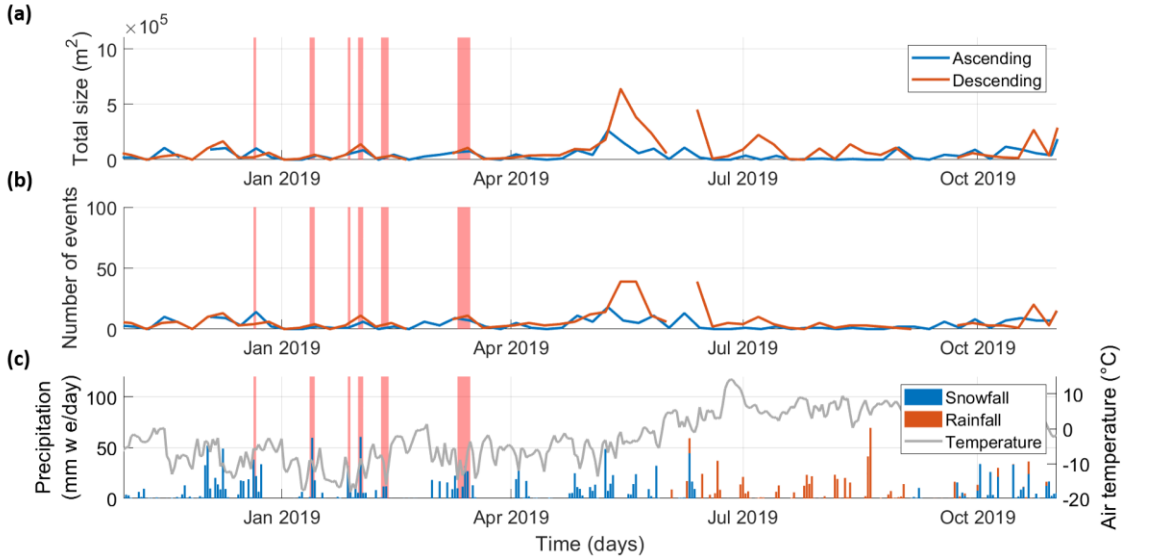

Figure S26: One year (11/2018-10/2019) of avalanche time series over the Mt Blanc massif in the ascending and descending orbits. (a) Total area and (b) number of avalanches as a function of time across all elevations. (c) Total daily precipitation and mean daily air temperature at 3000 m a.s.l over the Mt Blanc massif according to the SAFRAN reanalysis product (Vernay et al., 2022). The red shaded areas indicate days with a predicted avalanche danger level higher than or equal to 3 (Source: Météo-France).

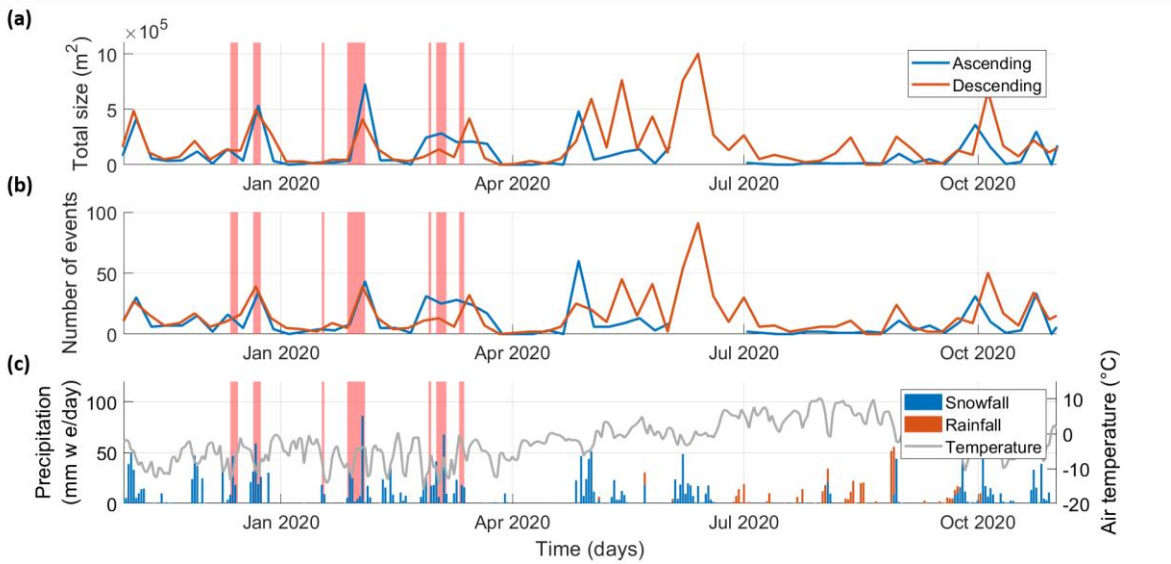

Figure S27: One year (11/2019-10/2020) of avalanche time series over the Mt Blanc massif in the ascending and descending orbits. (a) Total area and (b) number of avalanches as a function of time across all elevations. (c) Total daily precipitation and mean daily air temperature at 3000 m a.s.l over the Mt Blanc massif according to the SAFRAN reanalysis product (Vernay et al., 2022). The red shaded areas indicate days with a predicted avalanche danger level higher than or equal to 3 (Source: Météo-France).

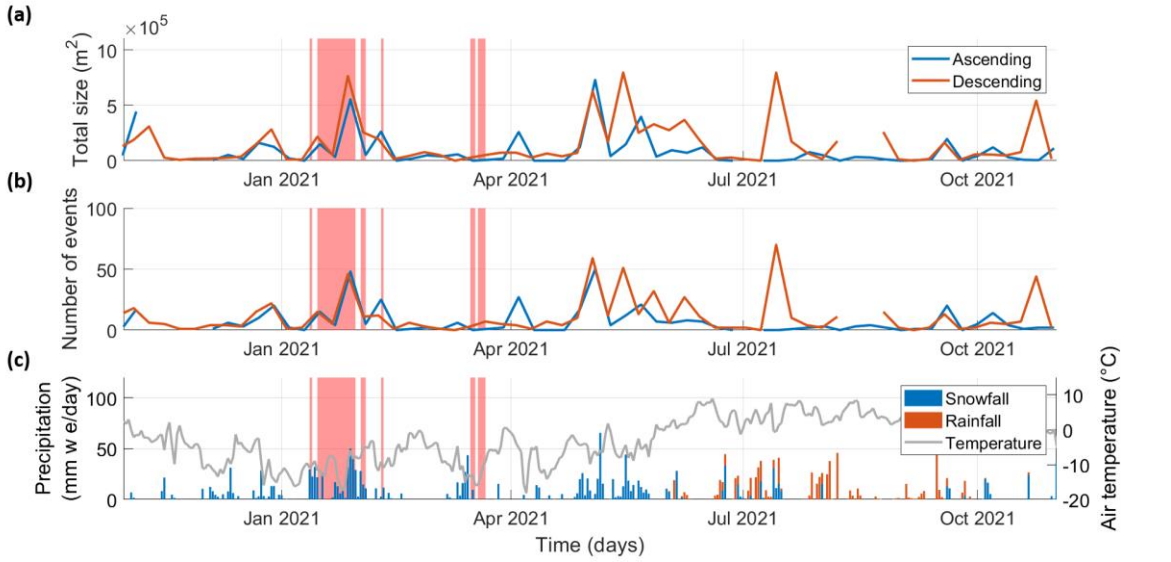

Figure S28: One year (11/2020-10/2021) of avalanche time series over the Mt Blanc massif in the ascending and descending orbits. (a) Total area and (b) number of avalanches as a function of time across all elevations. (c) Total daily precipitation and mean daily air temperature at 3000 m a.s.l over the Mt Blanc massif according to the SAFRAN reanalysis product (Vernay et al., 2022). The red shaded areas indicate days with a predicted avalanche danger level higher than or equal to 3 (Source: Météo-France).

Table S6: Total size of avalanches manually mapped over a given time period of 12 days, using images with a 6 days interval and a 12 days interval over the Mt Blanc study area.

Orbit	Time period	Area (px) - 6 days	Area (px) - 12 days	Ratio 12d/6d (%)
ASCENDING	06/02-18/02/20	781	704	90
	06/05-18/05/20	1934	1542	80
	04/08-16/08/20	206	106	51
	02/11-14/11/19	4682	3841	82
DESCENDING	05/02-17/02/20	1891	1058	56
	05/05-17/05/20	9195	3521	38
	03/08-15/08/20	3469	3343	96
	01/11-13/11/19	5979	3998	67

Table S7: F1-scores obtained for the calibration of our automated mapping method applied to VV and VH RGB triplets for the period 2019-2020 over the Mt. Blanc massif, and comparison with the scores obtained when averaging VV and VH (approach used in this study).

Polarisation	Path	Season	F1-score calibration
VV	Descending	November-April	0.29
		May-October	0.40
	Ascending	November-April	0.47
		May-October	0.31
VH	Descending	November-April	0.17
		May-October	0.18
	Ascending	November-April	0.14
		May-October	0.30
(VV+VH)/2	Descending	November-April	0.56
		May-October	0.56
	Ascending	November-April	0.54
		May-October	0.49